STANDARD ARTICLE

Journal of Veterinary Internal Medicine   ACVIM

Open Access   American College of Veterinary Internal Medicine

Association of sustained supraphysiologic hyperinsulinemia and inflammatory signaling within the digital lamellae in light-breed horses

Mauria R. Watts[1] | Olivia C. Hegedus[1] | Susan C. Eades[2] | James K. Belknap[1] [ORCID] |
Teresa A. Burns[1] [ORCID]

[1]Department of Veterinary Clinical Sciences, The Ohio State University College of Veterinary Medicine, Columbus, Ohio

[2]Department of Large Animal Clinical Sciences, Texas A&M University College of Veterinary Medicine and Biomedical Sciences, College Station, Texas

Correspondence
Teresa A. Burns, Department of Veterinary Clinical Sciences, The Ohio State University College of Veterinary Medicine, 601 Vernon Tharp Street, Columbus, OH 43210.
Email: burns.402@osu.edu

Abstract

Background: Hyperinsulinemia is associated with equine laminitis, and digital lamellar inflammation in equine metabolic syndrome-associated laminitis (EMSAL) is modest when compared with sepsis-associated laminitis.

Objectives: To characterize digital lamellar inflammation in horses in a euglycemic-hyperinsulinemic clamp (EHC) model of laminitis.

Animals: Sixteen healthy adult Standardbred horses.

Methods: Prospective experimental study. Horses underwent EHC or saline infusion (CON) for 48 hours or until the onset of Obel grade 1 laminitis. Horses were euthanized, and digital lamellar tissue was collected and analyzed via polymerase chain reaction (pro-inflammatory cytokine and chemokine genes—CXCL1, CXCL6, CXCL8, IL-6, MCP-1, MCP-2, IL-1β, IL11, cyclooxygenases 1 and 2, tumor necrosis factor alpha [TNF-α], E-selectin, and ICAM-1), immunoblotting (phosphorylated and total signal transducer and activator of transcription 1 [STAT1], STAT3, and p38MAPK), and immunohistochemistry (markers of leukocyte infiltration: CD163, MAC387).

Results: Lamellar mRNA concentrations of IL-1β, IL-6, IL-11, COX-2, and E-selectin were increased; the concentration of COX-1 was decreased; and concentrations of CXCL1, CXCL6, MCP-1, MCP-2, IL-8, TNF-α and ICAM-1 were not significantly different in the EHC group compared to the CON group ($P \leq .003$). Lamellar concentrations of phosphorylated STAT proteins (P-STAT1 [S727], P-STAT1 [Y701], P-STAT3 [S727], and P-STAT3 [Y705]) were increased in the EHC group compared to the CON group, with phosphorylated STAT3 localizing to nuclei of lamellar basal epithelial cells. There was no change in the lamellar concentration of P-p38 MAPK (T180/Y182), but the concentration of total p38 MAPK was decreased in the EHC samples. There was no evidence of notable lamellar leukocyte emigration.

Abbreviations: ABC, avidin-biotin complex; AMPK, 5′-adenosine monophosphate-activated protein kinase; BWE, black walnut extract; cDNA, complementary deoxyribonucleic acid; CHO, enteral carbohydrate overload; CON, control; COX1, cyclooxygenase-1; COX2, cyclooxygenase-2; CXCL1, C-X-C motif chemokine ligand-1; CXCL6, C-X-C motif chemokine ligand-6; CXCL8, C-X-C motif chemokine ligand-8; EHC, euglycemic-hyperinsulinemic clamp; EMSAL, equine metabolic syndrome-associated laminitis; EtOH, ethanol; HRP, horseradish peroxidase; ICAM-1, intercellular adhesion molecule-1; IF, immunofluorescence; IL-1β, interleukin-1β; IL-6, interleukin-6; IL-11, interleukin-11; MCP-1, monocyte chemoattractant protein-1; MCP-2, monocyte chemoattractant protein-2; mRNA, messenger ribonucleic acid; mTORC1, mammalian target of rapamycin complex-1; PCR, polymerase chain reaction; PMSF, phenylmethylsulfonyl fluoride; STAT1, signal transducer and activator of transcription-1; STAT3, signal transducer and activator of transcription-3; TBST, Tris-buffered saline plus Tween-20; TNF-α, tumor necrosis factor alpha.

Conclusions and Clinical Importance: These results establish a role for lamellar inflammatory signaling under conditions associated with EMSAL.

KEYWORDS

endocrinopathic, equine metabolic syndrome, immunology, inflammation, insulin, laminitis

1 | INTRODUCTION

Equine endocrinopathic laminitis, associated with conditions such as equine metabolic syndrome, pituitary pars intermedia dysfunction, and exogenous corticosteroid administration, is the most common type of laminitis encountered in equine veterinary practice.[1] Insulin dysregulation is likely the common variable among these conditions that most closely predicts the risk of laminitis[2–5]; further support for the role of insulin dysregulation in the pathophysiology of laminitis is provided by the ability of investigators to experimentally induce laminitis in clinically normal ponies and horses with sustained application of the euglycemic hyperinsulinemic clamp (EHC) technique.[6,7] Although parenteral infusion of supraphysiologic amounts of regular insulin and glucose is reliably associated with induction of laminitis under experimental conditions, the mechanisms linking these substrates to lamellar structural changes are presently unclear.

Inflammation is a component of many disease processes, including equine laminitis.[8–10] Inflammation has been clearly established as a component of the pathophysiology of sepsis-associated laminitis, and detailed descriptions of lamellar inflammatory events are reported for both the black walnut extract (BWE[11–13]) and enteral carbohydrate overload (CHO[10,13–15]) models (both of which are robustly inflammatory). However, even in these 2 inflammatory models, there is an inconsistent relationship between the presence and degree of inflammation and severity and outcome of disease. For example, although lamellar neutrophil infiltration is early and profound in the BWE model,[15,16] laminitis associated with this treatment can be transient and self-limiting if the exposure is not persistent or repeated. In contrast, lamellar leukocyte infiltration in horses subjected to the CHO model is primarily mononuclear and relatively late; laminitis in horses subjected to this model often proceeds to lamellar failure, even with a single enteral dose of wood/corn starch.[15] Therefore, there is established precedent for variability in the pathophysiological pathways that can lead to a similar ultimate lesion—dysadhesion of the lamellar basal epithelial cell from its underlying basement membrane, stretching of the epidermal lamellae, and displacement of the distal phalanx within the hoof capsule. Furthermore, establishing the relevance of inflammation to a particular clinical syndrome is important, as physical and pharmacological interventions to mitigate inflammation are well-accepted, widely used, and could be rationally incorporated into treatment protocols if a condition is inflammatory in nature.

The role of lamellar inflammation has been evaluated in naturally occurring and experimental models of insulin dysregulation and pasture-associated laminitis, with somewhat inconsistent results. In 1 report, mixed results regarding changes in lamellar concentrations of several inflammatory molecules in the EHC model led investigators to conclude that an innate inflammatory response did not play an important role in laminitis associated with hyperinsulinemia.[17] Additionally, little inflammatory signaling or leukocyte emigration into lamellar tissue has been reported when evaluating individuals with naturally occurring endocrinopathic laminitis[4,5] or those subjected to a dietary model intended to mimic risk factors for pasture-associated laminitis.[18] The purpose of this study was to characterize inflammatory signaling in lamellar tissue of adult horses subjected to an EHC model of equine metabolic syndrome-associated laminitis (EMSAL).

2 | MATERIALS AND METHODS

2.1 | Animal Protocol

Sixteen Standardbred horses were purchased from a private dealer for the study. No specific history was available regarding the animals' history of laminitis. The number of animals to be included in the study was selected based on the statistical analysis of data from previous studies in our laboratory in which this number of horses provided adequate statistical power when measuring similar outcomes.[10,18,19] The horses ranged from 4 to 18 years of age (mean 12.56 ± 4.4 years), and their body condition scores ranged from 4 to 7 out of 9 (mean 5.0 ± 1.0).[20] Horses showing any clinical signs of laminitis, including hoof capsule deformity or forelimb lameness at a walk (Obel grade 2[21,22]) were excluded from the study. All animals received humane treatment in accordance with an animal care and use protocol approved by The Ohio State University Institutional Animal Care and Use Committee.

All horses underwent a 14-day acclimation period in a barn stalled individually with ad libitum access to grass hay before the experimental protocol. The horses were then transported to a climate-controlled equine hospital, acclimatized for an additional 48 hours, and assigned randomly to either undergo an EHC (n = 8) or a sham infusion of saline (CON, n = 8) for 48 hours. After clipping, aseptic preparation of the overlying skin, and SC infusion of local anesthetic (2% lidocaine; Sparhawk Laboratories, Lenexa, Kansas), two 14-gauge intravenous catheters (Becton-Dickinson, Franklin Lakes, New Jersey) were aseptically placed into the left and right external jugular veins (1 catheter in each vein). The EHC protocol was then performed as previously described.[7,19] Briefly, blood was collected 3 times (10 minutes apart) to establish the mean baseline serum insulin and glucose concentrations. Insulin infusion was then initiated in the EHC group with a priming bolus (45 mIU/kg body weight [BW]) of regular insulin (Lily, LLC, Indianapolis, Indiana),

followed by a constant-rate infusion (Heska, Loveland, Colorado) of 6 mIU insulin/kg BW/min for the duration of the experiment (48 hours). Intravenous dextrose infusion was initiated immediately after administration of the bolus of insulin at a rate of 10 μmol/kg BW/min using 50% dextrose (Novatech, Inc, Grand Island, Nebraska) administered through the same catheter as the insulin infusion (separate infusion pump); the rate of dextrose infusion was adjusted to maintain blood glucose concentrations at 5.0 ± 1.0 mmol/L throughout the course of the experiment. Blood glucose was assessed every 5 minutes (via handheld glucometer; Roche Diagnostics, Indianapolis, Indiana) for the first 3 hours then every 30 minutes for the remainder of the experiment. After administration of the insulin bolus, blood was collected for subsequent determination of serum insulin and plasma glucose concentrations hourly for 8 hours, then every 2 hours for 4 hours, then every 5 hours for the remainder of the protocol. Horses in the CON group received a 0.9% saline infusion (Hospira, Lake Forest, Illinois) (0.57 mL/kg/h) for the duration of the experimental period; blood samples for measurement of glucose and insulin concentrations were collected every 6 hours from horses in the CON group.

All horses were monitored for lameness (at walk and trot) and foot pain (hoof tester application; Jorgenson Laboratories, Inc, Loveland, Colorado) every 2 hours starting after 24 hours of infusion. The animals were euthanized either at the onset of lameness (Obel Grade 1 lameness) or at 48 hours after the start of infusion, whichever occurred first. Lamellar tissue samples from the front and hind feet were obtained within 15 minutes of euthanasia and snap-frozen in liquid N_2, frozen in optimal cutting temperature compound (Sakura Finetek, Torrance, California) for cryo-sectioning for immunofluorescence (IF) analyses and fixed in 10% neutral buffered formalin (Fisher Scientific, Waltham, Massachusetts) for 48 hours (subsequently transferred to 70% ethanol [EtOH] for storage) for immunohistochemistry. Tissue from the CON front feet was used as a referent for comparisons with the EHC group.

2.2 | RNA isolation, complementary DNA synthesis, and quantitative real-time polymerase chain reaction

Three sections of frozen lamellar tissue from each sample were pulverized, and total RNA was isolated using a guanidine thiocyanate spin column method (Agilent Technologies, West Cedar, Texas) with a DNase digestion step included to eliminate any potential genomic DNA contamination. Messenger RNA (mRNA) was further purified with a poly-A tail streptavidin magnetic bead kit (Roche Diagnostics), and complementary DNA (cDNA) was synthesized from 400 ng mRNA. The cDNA was diluted at 1 : 5, 1 : 50, and 1 : 500 ratio and stored at −20°C until quantitative polymerase chain reaction (qPCR) was performed.

Quantitative real-time PCR was performed in the SYBR Green I format on a thermocycler (Roche LC 2.0; Roche Life Science, Indianapolis, Indiana). Each set of reactions containing samples from CON and EHC lamellae was run in duplicate and included double distilled H_2O as a negative control, controls without added reverse transcriptase, and a standard curve made from serial dilutions (10^1 to 10^6) of linearized vector containing the equine-specific gene sequence of interest. Primers for the following genes were synthesized based on published equine

genomic sequences using a commercial software program (DNASTAR, Madison, Wisconsin): C-X-C motif chemokine ligand 1 (CXCL1), CXCL6, CXCL8, interleukin 8 (IL-8), IL-6, monocyte chemoattractant protein 1 (MCP-1), MCP-2, IL-1β, IL-11, tumor necrosis factor alpha (TNF-α), cyclooxygenases 1 and 2 (COX-1 and COX-2), intercellular adhesion molecule 1 (ICAM-1), E-selectin, and the reference genes β-actin, β-2 microglobulin, glyceraldehyde-3 phosphate dehydrogenase, and TATA-box binding protein.

A commercially available software program (qbase+; Biogazelle, Zwijnaarde, Belgium) was used to identify the most stable reference genes from several candidate housekeeping genes evaluated in-run with the lamellar samples. The 2 genes identified as most stable and appropriate for reference with this sample set were β-actin and β-2 microglobulin. The geNorm algorithm calculates a normalization factor for samples from each animal based on the geometric mean of the chosen reference genes. Expression data for genes of interest are normalized by dividing the copy number data from each gene by this normalization factor. The data are reported as either absolute copy number or fold-change from control values (calculated by dividing the normalized EHC expression values by the normalized CON values for each gene).

2.3 | Protein extraction

Protein was extracted from snap-frozen lamellar samples as previously described.[13,19] Briefly, all samples underwent an initial pulverization step before homogenization on ice in a commercially available lysis buffer (Thermo Scientific, Waltham, Massachusetts) with the addition of protease and phosphatase inhibitors and phenylmethylsulfonyl fluoride (PMSF). Samples were then incubated on ice for 30 minutes. The supernatant was separated by centrifugation and collected, and protein concentration was quantified using the Bradford method. Protein samples were stored at −80°C until analysis.

2.4 | Immunoblotting

The lamellar concentrations of phospho-proteins of interest were assessed as previously described[13,19] via Western immunoblot analysis of lamellar samples using commercially available antibodies raised against signal transducer and activator of transcription 1 (STAT1) P-(S727), STAT1 P-(Y701), STAT3 P-(S727), STAT3 P-(Y705), and p38 mitogen activated protein kinase P-(T180/Y182). Total protein concentrations were assessed using antibodies recognizing the protein of interest without respect to its phosphorylation state. Finally, β-actin protein concentrations were assessed as a loading control in all samples for normalization of results (Santa Cruz Biotechnology, Inc, Dallas, Texas). All antibodies except β-actin were obtained from a single source (Cell Signaling Technology, Inc, Danvers, Massachusetts). Briefly, lamellar protein samples (20 μg) were denatured by boiling in SDS/β-ME buffer (Bio-Rad; Hercules, California) for 5 minutes, separated by electrophoresis on a polyacrylamide gel (Bio-Rad) and transferred to a polyvinylidene fluoride membrane (Bio-Rad). The membrane was blocked in 5% milk (Bio-Rad) in Tris-buffered saline plus Tween-20

(0.1% vol/vol Tween 20; TBST; Thermo Scientific) for 1 hour at room temperature, rocking. The membrane was then incubated with primary antibody against the phospho-protein of interest at 4°C overnight. The membrane was then washed 3 times in 0.1% TBST and incubated with the appropriate IgG horseradish peroxide (HRP)-conjugated secondary antibody for 1 hour at room temperature, rocking. The membrane was washed in 0.1% TBST, and signal was developed with a chemiluminescent substrate (Thermo Scientific). The membrane was then stripped with a commercially available buffer (Thermo Scientific) and re-probed sequentially for the corresponding total protein and β-actin. Luminescence was measured using a computer software program (US National Institutes of Health, Bethesda, Maryland), and the signal strength was determined by dividing the net intensity of the phospho-protein (or total protein) band by that of the β-actin band.

2.5 | Immunofluorescence

Ten micrometer cryosections of lamellar tissue were fixed in 4% formaldehyde (Polysciences, Inc, Warrington, Pennsylvania) for 15 minutes at room temperature, cell membranes were permeabilized with ice-cold methanol (Fisher Scientific, Waltham, Massachusetts) for 20 minutes at −20°C, and sections were blocked with 5% goat serum (Cell Signaling Technology, Inc.) in a phosphate-buffered saline solution containing 3% Tween-20 for 1 hour at room temperature. The slides were incubated overnight with a rabbit monoclonal antibody against P-STAT3 (Y705) (used at a 1:100 dilution) and a mouse monoclonal antibody against total STAT3 (used at a 1:1500 dilution) (Cell Signaling Technology, Inc). After washing, the slides were incubated at room temperature for 1.5 hours in an anti-rabbit monoclonal antibody conjugated with Alexa Fluor 555 (Cell Signaling Technology, Inc) (1:200 dilution) and an anti-mouse monoclonal conjugated with Alexa Fluor 647 (1:500 dilution), then with the DNA-intercalating dye 4′,6-diamidino-2-phenylindole (Cell Signaling Technology, Inc); coverslips were applied, and the sections were digitally imaged using a laser assisted confocal microscope (Olympus, Center Valley, Pennsylvania).

2.6 | Immunohistochemistry

Leukocyte emigration into digital lamellar tissue was assessed with MAC387/calprotectin and CD163 immunohistochemical staining using the avidin-biotin complex (ABC) method as previously described.[12,15,16,23] Briefly, 5-μm tissue sections were prepared from formalin-fixed, paraffin-embedded lamellar tissue and affixed to slides. The sections were deparaffinized sequentially in EtOH (70%-100%), antigen was unmasked with 20 μg/mL proteinase-K (Thermo Scientific) applied for 6 minutes at room temperature, and endogenous peroxidase activity was quenched in 3% hydrogen peroxide for 10 minutes. Nonspecific binding was blocked with a solution containing normal goat serum (2%) and bovine serum albumin (2.5%) (Jackson ImmunoResearch Laboratories, Inc, West Grove, Pennsylvania). The tissue sections were incubated at 4°C overnight with a MAC387 mouse monoclonal antibody (1:250 dilution) (Abcam, Cambridge, Massachusetts); after washing, the samples were

incubated for 1 hour in a 1:100 dilution of a biotinylated secondary antibody (Vector Laboratories, Burlingame, California), then subsequently incubated in ABC reagent (Vector Laboratories) for 30 minutes in the dark at room temperature. The sections were incubated for 6 minutes in DAB chromogen (Vector Laboratories) to develop signal, counterstained with hematoxylin, and sealed with a coverslip. Sections were stained similarly for CD163 (TransGenic, Inc, Fukuoka, Japan), with the exception that the antigen retrieval procedure was performed with sodium citrate (Thermo Scientific), and the samples were processed with an automated slide system (Dako/Agilent Technologies, West Cedar, Texas). Two blinded investigators (MRW, JKB) assessed the number of lamellar MAC387- and CD163-positive cells, with each observer counting n = 10 40× fields per slide.

2.7 | Data analysis

The RT-qPCR data from 2 housekeeping genes (β-actin and β_2-microglobulin) were entered into a commercially available computer program to test each gene's suitability as a housekeeping gene for the equine lamellar tissue samples. Because both genes were determined to be satisfactory, a geometric mean was obtained from the 2 genes' data to generate a normalization factor for gene expression from each

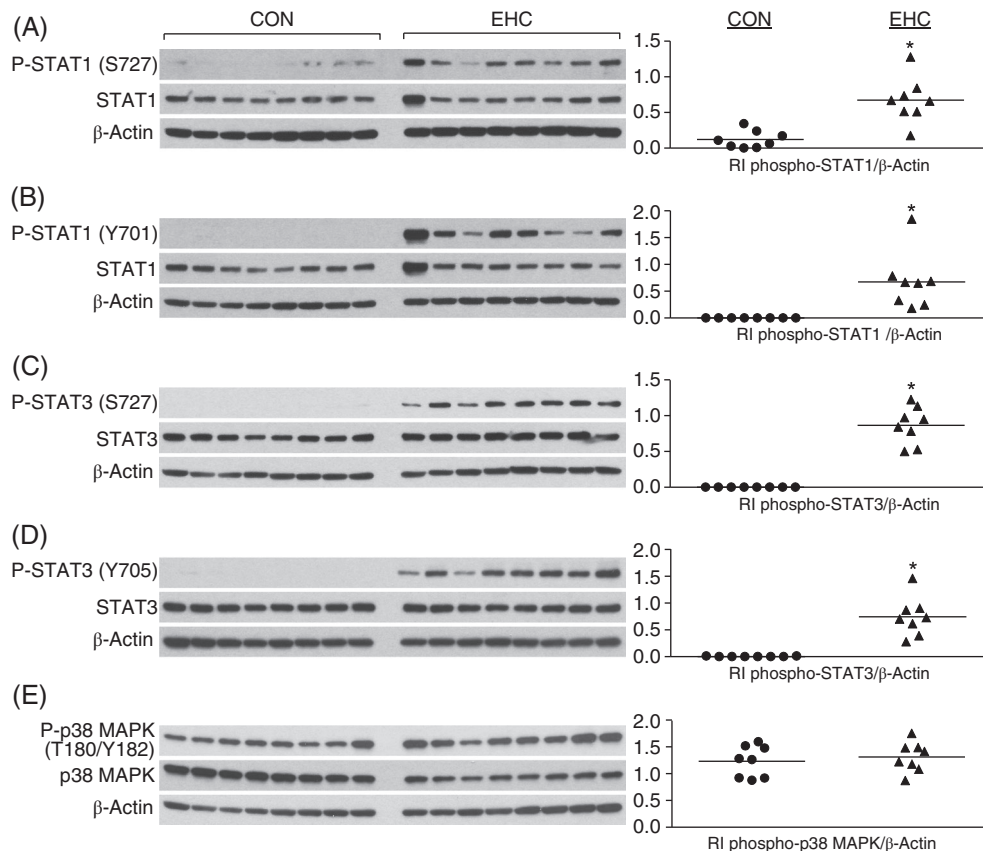**TABLE 1** Real-time quantitative PCR copy number data

Gene	CON	EHC	Fold change	P value
COX-1	1.00 ± 0.28	0.38 ± 0.14	↓0.38	**<.001**
COX-2	1.00 ± 0.27	42.93 ± 28.92	↑**42.93**	.001
CXCL1[a]	0.89 (0.68-1.17)	1.04 (0.75-2.79)	↑1.64	.44
CXCL6	1.00 ± 0.45	2.10 ± 1.40	↑ 2.09	.05
CXCL8 (IL-8)	1.00 ± 0.40	22.01 ± 25.71	↑22.01	.04
E-selectin	1.00 ± 0.66	2.76 ± 1.06	↑**2.76**	**.001**
ICAM-1	1.00 ± 0.32	1.16 ± 0.54	↑1.76	.47
IL-1β	1.00 ± 0.19	1.84 ± 0.77	↑**1.84**	.009
IL-6	1.00 ± 0.38	178.7 ± 140.6	↑**178.69**	.003
IL-11[a]	1.04 (0.78-1.26)	8.90 (3.42-28.06)	↑**16.29**	**<.001**
MCP-1[a]	400 (316.3-561.5)	2005 (1358-3183)	↑5.40	.01
MCP-2[a]	1.03 (0.63-1.24)	1.13 (1.01-1.46)	↑1.26	.38
TNF-α	1.00 ± 0.10	0.75 ± 0.29	↓0.75	.04

Normally distributed data evaluated with Student's *t*-test, presented as mean ± SD. Fold change calculated as EHC/average CON for each gene of interest.

A Bonferroni adjustment for multiple comparisons suggested that statistical significance should be accepted at $P \leq 0.003$.

Values in bold type are those that are significantly different between the CON and EHC groups ($P \leq 0.003$).

[a]Non-normally distributed data evaluated with Mann-Whitney *U* test, presented as median (25%–75% interquartile range).

WATTS ET AL.

Journal of Veterinary Internal Medicine ACVIM

Open Access

American College of
Veterinary Internal Medicine

| 1487

FIGURE 1 Western immunoblot data evaluating lamellar concentrations of phosphorylated and total STAT1 protein (A and B), STAT3 protein (C and D), and p38 MAPK protein (E) in control horses (CON) and those subjected to an EHC model of laminitis. Horses in the EHC group had greater lamellar concentrations of P-STAT1 (S727 [A] and Y701 [B]) and P-STAT3 (S727 [C] and Y705 [D]) than those in the CON group ($P < .05$). There was no difference in lamellar concentration of P-p38 MAPK (T180/Y182; E) between the CON and EHC groups ($P > .05$); however, horses in the EHC group had significantly lower lamellar concentrations of total p38 MAPK than those in the CON group ($P < .05$). CON, control; EHC, euglycemic-hyperinsulinemic clamp; MAPK, mitogen activated protein kinase; P-p38 MAPK, phosphorylated p38 MAPK; P-STAT, phosphorylated STAT; RI, relative band intensity; STAT1, signal transducer and activator of transcription

sample. Gene expression data from the genes of interest were then normalized using the factor unique to each sample.

Data analysis was performed using a statistical software program (GraphPad Software, Inc, La Jolla, California). All data were assessed for normality by the Shapiro-Wilk and D'Agostino and Pearson omnibus normality tests. Laminar leukocyte quantification, mRNA concentration, and protein concentration data were analyzed with a Student's t test (or nonparametric equivalent as appropriate). For the mRNA concentration data, a Bonferroni correction for multiple comparisons suggested that statistical significance should accepted at $P < .003$; elsewhere, statistical significance was accepted at $P ≤ .05$. Data are expressed as mean ± SD unless otherwise indicated.

3 | RESULTS

3.1 | EHC model

Details regarding the animal-level outcomes of this experimental EHC model, including concentrations of serum insulin and plasma glucose measured during the protocol, have been published.[19]

3.2 | Real-time qPCR

Real-time qPCR was performed to measure lamellar mRNA concentrations of selected inflammatory mediators. Lamellar mRNA concentrations of IL-1β, IL-6, IL-11, COX-2, and E-selectin were increased in the EHC group compared to the CON group; the concentration of COX-1 was decreased in the EHC group compared to the CON group ($P ≤ .003$). Lamellar mRNA concentrations of CXCL1, CXCL6, MCP-1, MCP-2, IL-8, TNF-α, and ICAM-1 were not significantly different between samples from EHC and CON animals ($P > .003$; Table 1).

3.3 | Western immunoblotting

Lamellar concentrations of phosphorylated STAT proteins (P-STAT1 [S727], P-STAT1 [Y701], P-STAT3 [S727], and P-STAT3 [Y705]) were increased in samples from the EHC group when compared with lamellar samples from the CON group ($P ≤ .0004$; Figure 1). There was no difference in P-p38 MAPK concentration between the groups (T180/Y182; Figure 1). The concentration of total p38 MAPK protein was decreased in the EHC lamellar samples when compared to the CON lamellae

TABLE 2 Western immunoblot relative intensity data for concentrations of phosphorylated and total signal proteins (STAT1, STAT3, and p38MAPK)

	CON	EHC	P-value
Lamellar phosphorylated signal protein concentrations			
P-STAT1 (S727)	0.120 ± 0.122	0.673 ± 0.316	**<.001**
P-STAT1 (Y701)[a]	1.0×10^{-4} $(1.0 \times 10^{-4}$- $1.0 \times 10^{-4})$	0.657 (0.265-0.755)	**<.001**
P-STAT3 (S727)	1.37×10^{-4} ± 5.17×10^{-5}	0.869 ± 0.261	**<.001**
P-STAT3 (Y705)	0.0031 ± 0.006	0.740 ± 0.360	**<.001**
P-p38 MAPK (T180/Y182)[a]	1.277 (0.923-1.606)	1.115 (1.326-1.494)	.58
Lamellar total signal protein concentrations			
STAT1 (for S727)[a]	0.849 (0.710-1.055)	0.814 (0.676-0.994)	.80
STAT1 (for Y701)[a]	0.625 (0.503-0.770)	0.569 (0.465-0.644)	.57
STAT3 (for S727)[a]	1.009 (0.742-1.33)	1.201 (1.124-1.324)	.32
STAT3 (for Y705)[a]	0.892 (0.869-1.007)	1.057 (0.872-1.203)	.38
p38 MAPK[a]	1.468 (1.107-2.024)	0.629 (0.564-0.761)	**<.001**

Western immunoblot relative intensity data assessed with an unpaired *t* test. Normally distributed data presented as mean ± SD. Statistical significance accepted at $P \leq .05$.
Values in bold type are those that are significantly different between the CON and EHC groups ($P \leq 0.003$).
[a]Non-normally distributed data analyzed with a Mann-Whitney *U* test and presented as median and (25%–75%) interquartile range.

(P = .002). There was no difference in the concentration of either of the total STAT proteins between the EHC and CON groups (Table 2).

3.4 | Correlations

Significant positive correlations were observed between concentrations of multiple pro-inflammatory transcripts and phosphorylated STAT and p38 MAPK proteins within the digital lamellae of horses experiencing prolonged hyperinsulinemia (Supporting information Supplemental Data 1).

3.5 | Leukocyte emigration

The number of lamellar MAC387+ cells was increased in samples from the EHC group when compared to the CON samples (P = .04), whereas the number of CD163+ cells within the lamellae was not different between the groups (P = .60; Figure 2).

3.6 | Immunofluorescence

Immunofluorescence was used to assess cellular localization of P-STAT3 (Y705). The phosphorylated form of STAT3 was localized near the nuclei
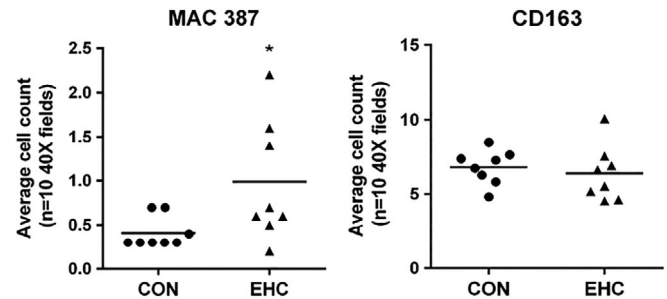
FIGURE 2 Lamellar MAC387(+) and C163(+) cell counts in control horses (CON) and those subjected to a euglycemic-hyperinsulinemic clamp model of laminitis (EHC). The number of MAC387(+) cells was greater in lamellae of horses in the EHC group compared to the CON group (P < .05), whereas the number of CD163(+) cells was not different between the groups (P > .05). The majority of MAC387(+) cells identified were epithelial cells

of lamellar basal epithelial cells and was markedly increased in samples from the EHC group when compared to those from the CON group. Total STAT3 was detected at similar levels in the lamellar tissue from both groups (Figure 3).

4 | DISCUSSION

The results of this study provide evidence of inflammatory signaling within the digital lamellae of light-breed horses experiencing prolonged supraphysiologic hyperinsulinemia. That said, it seems unlikely that this signaling represents established, "classic" inflammation as a primary pathophysiologic mechanism involved in endocrinopathic laminitis, since in agreement with previous reports, little to no evidence of leukocyte emigration into lamellar tissue was observed in response to this model (that emigration being a hallmark of inflammation). Rather, the lamellar inflammatory signaling observed here may instead be an evidence of cross-talk between metabolic regulatory signaling pathways and inflammatory pathways occurring in response to altered intracellular concentrations of energetic metabolites, which has been documented to occur in multiple cell types in vitro and in vivo.[24–27]

Laminitis that occurs in equine patients with systemic insulin dysregulation and hyperinsulinemia is likely to be associated with disordered nutrient sensing and metabolism within the digital lamellae.[28–30] Molecular mechanisms for nutrient and energetic sensing are highly conserved among eukaryotic organisms[31]; 2 centrally important signaling pathways linking nutrient substrate flux to cellular processes (such as differentiation, proliferation, intercellular adhesion, inflammation, etc.) are mammalian target of rapamycin complex-1 (mTORC1) signaling[24,32] and adenosine 5′-monophosphate-activated protein kinase (AMPK) signaling.[33] These important energy sensors are typically regulated in opposing directions, with mTORC1 signaling activated during times of increased substrate availability (glucose, amino acids) and AMPK signaling activated during energetic stress (high intracellular AMP to ATP ratio); they therefore classically signal opposing cellular energetic states.[24] Both mTORC1 and AMPK signaling intersect at various nodes with inflammatory pathways, integrating metabolic signals with

FIGURE 3 Immunofluorescence for lamellar STAT3 and P-STAT3 in tissue from horse subjected to an EHC model of laminitis (EHC [A, B, C, D]; ×60 magnification) and a control horse (CON [E, F, G, H]; ×40 magnification). Panels A and E (red), total STAT3; panels B and F (green), P-STAT3 (Y705); panels C and G (blue), DAPI; panels D and H, overlay. Lamellar P-STAT3 concentration was increased in lamellae from the EHC group compared to CON, and total and P-STAT3 showed nuclear localization in tissue from the EHC group. CON, control; DAPI, 4′, 6-diamidino-2-phenylindole; EHC, euglycemic-hyperinsulinemic clamp; P-STAT3, phosphorylated STAT3; STAT3, signal transducer and activator of transcription-3
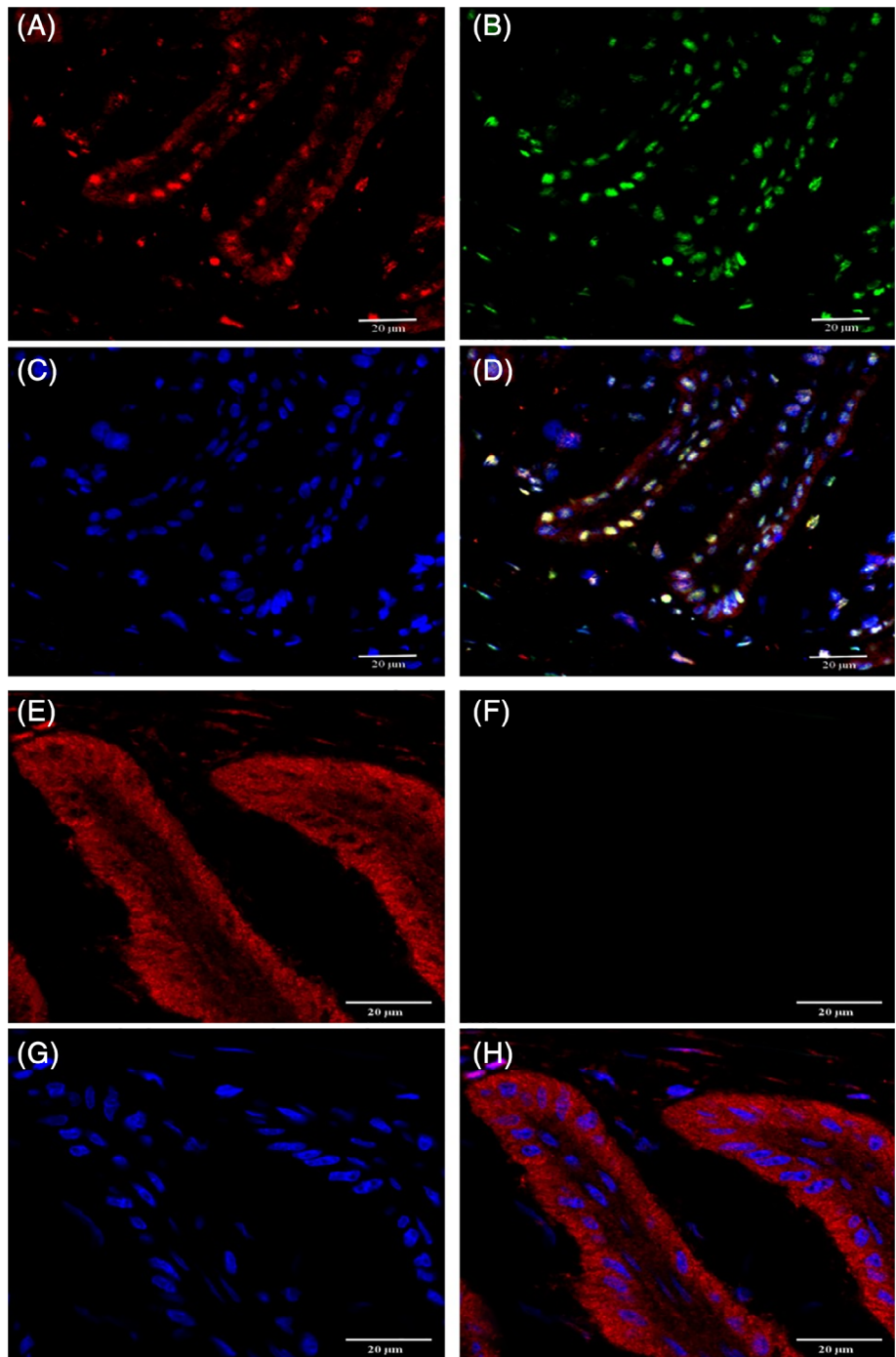
those governing inflammatory responses.[24,34,35] Interestingly, although evidence of activation of mTORC1 signaling in the digital lamellae has been documented in this model,[19] we found no evidence of altered AMPK activation in the same tissue. This could be explained based on the competing influences on AMPK activation that may be present at the cellular level under these experimental conditions; increased glucose availability is well known to decrease AMPK activation,[36] but leptin has been reported to increase AMPK activity through JAK2 signaling.[37] Interestingly, even if AMPK activation is not regulated primarily in this model, pharmacologic activation of AMPK may still be useful therapeutically under these circumstances, as activation of AMPK

results in direct and indirect inhibition of mTORC1.[24] As AMPK agonists are already in regular clinical use in equine veterinary medicine,[38–41] further investigation of these agents in the treatment of EMSAL seems warranted.

Signal transducer and activation of transcription signaling has been described in lamellar tissue from horses subjected to models of sepsis-associated laminitis (both BWE and CHO models), with activating phosphorylation of STAT3 reported at both developmental and OG1 time points in sepsis-associated disease.[13] Activating phosphorylation of lamellar STAT1 was not observed in these models, which was suggested to be due to lack of local interferon expression during

disease development.[13] Uniquely, here we report activation of both STAT3 (similar to sepsis-associated laminitis) and STAT1 in lamellar tissue from horses experiencing sustained supraphysiologic hyperinsulinemia. Activation of STAT1 and STAT3 as a result of activation of a single intracellular signaling pathway is uncommon but has been reported to occur in limited instances in other tissues/cell types; an important example that may have relevance for obesity-related laminitis is activation of STAT1 and STAT3 after ligand binding and activation of long-form leptin receptor.[42] Keratinocytes express leptin receptor in other species,[43] and serum leptin concentrations have been reported to increase significantly in a matter of hours in young, healthy humans in response to induced hyperinsulinemia.[44,45] Although the results of the study reported here cannot verify the importance of leptin signaling in EHC-induced laminitis, given the evidence established in other species (and the fact that overweight/obese equids at risk for EMSAL are likely to be hyperleptinemic[46–48]), further investigation of this mechanism seems warranted.

A curious finding of this study was the significant downregulation of p38 MAPK total protein in lamellar tissue of horses subjected to the EHC. Function of the diverse members of the MAPK family is almost exclusively regulated through control of phosphorylation events by kinases and phosphatases, and little information exists regarding their regulation at the transcript or protein levels.[49] However, in certain specific circumstances, changes in expression, posttranslational modifications (such as acetylation), incorporation into intracellular scaffold structures, and modification of proteolysis are known to affect the p38 MAPK pathway and might be relevant to the pathophysiology of equine disease.[49] Further study is needed in this area to determine the importance of this finding, although it could represent a regulatory feedback response to activation of inflammatory signaling pathways in this setting.

The lack of significant lamellar inflammatory cell infiltrates accompanying this model suggests that the source of pro-inflammatory cytokines and chemokines detected within lamellar tissue is likely to be the major cell type in this tissue, the lamellar keratinocyte. Both human and equine keratinocytes produce pro-inflammatory cytokines and chemokines when stimulated with various pathogen-associated molecular pattern molecules in vitro,[50] and these cells likely have the capacity to elaborate these substances in vivo in response to various stimuli as well (including exposure to elevated leptin concentrations[51]). Although evaluating mRNA concentrations alone is useful to identify the activation of inflammatory signaling pathways in general, determining the role of the individual cytokines/chemokines involved would necessitate quantification of the native peptides/proteins as well in some way (immunoblotting, IF, flow cytometry, etc.), which is a limitation of the current study. However, based on the results of this work, it seems clear that inflammatory signaling within the lamellae, possibly elicited through exposure to increased concentrations of glucose, insulin (acting through insulin receptor and/or IGF-1 receptor), leptin, or other metabolic intermediates, is observed under conditions that induce lesions of EMSAL. Future work should aim to clarify the role this signaling plays in EMSAL pathophysiology, particularly as it relates to lamellar basal epithelial cell function and lamellar failure.

CONFLICT OF INTEREST DECLARATION

Authors declare no conflict of interest.

OFF-LABEL ANTIMICROBIAL DECLARATION

Authors declare no off-label use of antimicrobials.

INSTITUTIONAL ANIMAL CARE AND USE COMMITTEE (IACUC) OR OTHER APPROVAL DECLARATION

The Ohio State University IACUC approved, #2015A0014.

HUMAN ETHICS APPROVAL DECLARATION

Authors declare human ethics approval was not needed for this study.

ORCID

James K. Belknap https://orcid.org/0000-0003-0345-8220
Teresa A. Burns https://orcid.org/0000-0001-9716-3452

REFERENCES

1. American Association of Equine Practitioners. AAEP membership equine research study report. www.aaepfoundation.org. Updated 2009. Accessed March 14, 2011.
2. Treiber KH, Kronfeld DS, Geor RJ. Insulin resistance in equids: possible role in laminitis. *J Nutr*. 2006;136(7 Suppl):2094S-2098S.
3. Carter RA, Treiber KH, Geor RJ, Douglass L, Harris PA. Prediction of incipient pasture-associated laminitis from hyperinsulinaemia, hyperleptinaemia and generalised and localised obesity in a cohort of ponies. *Equine Vet J*. 2009;41(2):171-178.
4. Karikoski NP, Patterson-Kane JC, Singer ER, McFarlane D, McGowan CM. Lamellar pathology in horses with pituitary pars intermedia dysfunction. *Equine Vet J*. 2016;48(4):472-478.
5. Karikoski NP, McGowan CM, Singer ER, Asplin KE, Tulamo RM, Patterson-Kane JC. Pathology of natural cases of equine endocrinopathic laminitis associated with hyperinsulinemia. *Vet Pathol*. 2015;52(5):945-956.
6. Asplin KE, Sillence MN, Pollitt CC, McGowan CM. Induction of laminitis by prolonged hyperinsulinaemia in clinically normal ponies. *Vet J*. 2007;174(3):530-535.
7. de Laat MA, McGowan CM, Sillence MN, Pollitt CC. Equine laminitis: induced by 48 h hyperinsulinaemia in standardbred horses. *Equine Vet J*. 2010;42(2):129-135.

8. Leise BS, Faleiros RR, Watts M, Johnson PJ, Black SJ, Belknap JK. Hindlimb laminar inflammatory response is similar to that present in forelimbs after carbohydrate overload in horses. *Equine Vet J*. 2012; 44(6):633-639.

9. Faleiros RR, Leise BS, Watts M, Johnson PJ, Black SJ, Belknap JK. Laminar chemokine mRNA concentrations in horses with carbohydrate overload-induced laminitis. *Vet Immunol Immunopathol*. 2011;144(1–2): 45-51.

10. Leise BS, Faleiros RR, Watts M, Johnson PJ, Black SJ, Belknap JK. Laminar inflammatory gene expression in the carbohydrate overload model of equine laminitis. *Equine Vet J*. 2011;43(1):54-61.

11. Belknap JK. Black walnut extract: an inflammatory model. *Vet Clin North Am Equine Pract*. 2010;26(1):95-101.

12. Faleiros RR, Nuovo GJ, Flechtner AD, Belknap JK. Presence of mononuclear cells in normal and affected laminae from the black walnut extract model of laminitis. *Equine Vet J*. 2011;43(1):45-53.

13. Leise BS, Watts M, Tanhoff E, Johnson PJ, Black SJ, Belknap JK. Laminar regulation of STAT1 and STAT3 in black walnut extract and carbohydrate overload induced models of laminitis. *J Vet Intern Med*. 2012;26(4):996-1004.

14. Pollitt CC, Visser MB. Carbohydrate alimentary overload laminitis. *Vet Clin North Am Equine Pract*. 2010;26(1):65-78.

15. Faleiros RR, Johnson PJ, Nuovo GJ, Messer NT, Black SJ, Belknap JK. Laminar leukocyte accumulation in horses with carbohydrate overload-induced laminitis. *J Vet Intern Med*. 2011;25(1):107-115.

16. Faleiros RR, Nuovo GJ, Belknap JK. Calprotectin in myeloid and epithelial cells of laminae from horses with black walnut extract-induced laminitis. *J Vet Intern Med*. 2009;23(1):174-181.

17. de Laat MA, Clement CK, McGowan CM, Sillence MN, Pollitt CC, Lacombe VA. Toll-like receptor and pro-inflammatory cytokine expression during prolonged hyperinsulinaemia in horses: implications for laminitis. *Vet Immunol Immunopathol*. 2014;157(1–2):78-86.

18. Burns TA, Watts MR, Weber PS, McCutcheon LJ, Geor RJ, Belknap JK. Laminar inflammatory events in lean and obese ponies subjected to high carbohydrate feeding: implications for pasture-associated laminitis. *Equine Vet J*. 2015;47(4):489-493.

19. Lane HE, Burns TA, Hegedus OC, et al. Lamellar events related to insulin-like growth factor-1 receptor signalling in two models relevant to endocrinopathic laminitis. *Equine Vet J*. 2017;49(5):643-654.

20. Henneke DR, Potter GD, Kreider JL, Yeates BF. Relationship between condition score, physical measurements and body fat percentage in mares. *Equine Vet J*. 1983;15(4):371-372.

21. Menzies-Gow NJ, Stevens KB, Sepulveda MF, Jarvis N, Marr CM. Repeatability and reproducibility of the obel grading system for equine laminitis. *VetRec*. 2010;167:52-55.

22. Obel N. Studies on the Histopathology of Acute Laminitis [dissertation]. Uppsala, Sweden: Almqvist & Wiksell Boktryckeri; 1948.

23. Godman JD, Burns TA, Kelly CS, et al. The effect of hypothermia on influx of leukocytes in the digital lamellae of horses with oligofructose-induced laminitis. *VetImmunolImmunopathol*. 2016;178(Oct 1):22-28.

24. Li H, Lee J, He C, Zou MH, Xie Z. Suppression of the mTORC1/STAT3/Notch1 pathway by activated AMPK prevents hepatic insulin resistance induced by excess amino acids. *Am J Physiol Endocrinol Metab*. 2014;306(2):E197-E209.

25. Tang T, Zhang J, Yin J, et al. Uncoupling of inflammation and insulin resistance by NF-kB in transgenic mice through elevated energy expenditure. *J Biol Chem*. 2010;285(7):4637-4644.

26. Lihn AS, Pedersen SB, Lund S, Richelsen B. The anti-diabetic AMPK activator AICAR reduces IL-6 and IL-8 in human adipose tissue and skeletal muscle cells. *Mol Cell Endocrinol*. 2008;292(1–2):36-41.

27. Stofkova A. Leptin and adiponectin: from energy and metabolic dysbalance to inflammation and autoimmunity. *Endocr Regul*. 2009;43(4):157-168.

28. Burns TA, Watts MR, Weber PS, McCutcheon LJ, Geor RJ, Belknap JK. Effect of dietary nonstructural carbohydrate content on activation of 5′-adenosine monophosphate-activated protein kinase in liver, skeletal muscle, and digital laminae of lean and obese ponies. *J Vet Intern Med*. 2014;28(4):1280-1288.

29. de laat MA, Clement CK, Sillence MN, McGowan CM, Pollitt CC, Lacombe VA. The impact of prolonged hyperinsulinemia on glucose transport in equine skeletal muscle and digital lamellae. *Equine Vet J*. 2015;47(4):494-501.

30. Asplin KE, Curlewis JD, McGowan CM, Pollitt CC, Sillence MN. Glucose transport in the equine hoof. *Equine Vet J*. 2011;43(2):196-201.

31. Hardie DG. AMP-activated/SNF1 protein kinases: conserved guardians of cellular energy. *Nat Rev Mol Cell Biol*. 2007;8(10):774-785.

32. Mounier R, Lantier L, Leclerc J, Sotiropoulos A, Foretz M, Viollet B. Antagonistic control of muscle cell size by AMPK and mTORC1. *Cell Cycle*. 2011;10(16):2640-2646.

33. Hardie DG. Adenosine monophosphate-activated protein kinase: a central regulator of metabolism with roles in diabetes, cancer, and viral infection. *Cold Spring Harb Symp Quant Biol*. 2011;76:155-164.

34. Henry WS, Laszewski T, Tsang T, et al. Aspirin suppresses growth in PI3K-mutant breast cancer by activating AMPK and inhibiting mTORC1 signaling. *Cancer Res*. 2017;77(3):790-801.

35. O'Neill LA, Hardie DG. Metabolism of inflammation limited by AMPK and pseudo-starvation. *Nature*. 2013;493(7432):346-355.

36. Towler MC, Hardie DG. AMP-activated protein kinase in metabolic control and insulin signaling. *Circ Res*. 2007;100(3):328-341.

37. Uotani S, Abe T, Yamaguchi Y. Leptin activates AMP-activated protein kinase in hepatic cells via a JAK2-dependent pathway. *Biochem Biophys Res Commun*. 2006;351(1):171-175.

38. Rendle DI, Rutledge F, Hughes KJ, Heller J, Durham AE. Effects of metformin hydrochloride on blood glucose and insulin responses to oral dextrose in horses. *Equine Vet J*. 2013;45(6):751-754.

39. Durham AE. Metformin in equine metabolic syndrome: an enigma or a dead duck? *Vet J*. 2012;191(1):17-18.

40. Watts AE, Dabareiner R, Marsh C, Carter GK, Cummings KJ. A randomized, controlled trial of the effects of resveratrol administration in performance horses with lameness localized to the distal intertarsal joints. *J Am Vet Med Assoc*. 2016;249(6):650-659.

41. Durham AE, Rendle DI, Newton JE. The effect of metformin on measurements of insulin sensitivity and beta cell response in 18 horses and ponies with insulin resistance. *Equine Vet J*. 2008;40(5):493-500.

42. Procaccini C, De Rosa V, Galgani M, et al. Role of adipokines signaling in the modulation of T cells function. *Front Immunol*. 2013;4(332): 1-12.

43. Tadokoro S, Ide S, Tokuyama R, et al. Leptin promotes wound healing in the skin. *PLoS One*. 2015;10(3):e0121242.

44. Faraj M, Beauregard G, Tardif A, et al. Regulation of leptin, adiponectin and acylation-stimulating protein by hyperinsulinemia and hyperglycemia in vivo in healthy young men. *Diabetes Metab*. 2008;34(4 [Pt 1]):334-342.

45. Schmitz O, Fisker S, Orskov L, Hove KY, Nyholm B, Moller N. Effects of hyperinsulemia and hypoglycemia on circulating leptin levels in healthy lean males. *Diabetes Metab*. 1997;23(1):80-83.

46. Schultz N, Geor RJ, Manfredi JM. Factors associated with leptin and adiponectin concentrations in a large across breed cohort of horses and ponies. *J Vet Intern Med*. 2014;28:998.

47. Pleasant RS, Suagee JK, Thatcher CD, Elvinger F, Geor RJ. Adiposity, plasma insulin, leptin, lipids, and oxidative stress in mature light breed horses. *J Vet Intern Med*. 2013;27(3):576-582.

48. Bamford NJ, Potter SJ, Harris PA, Bailey SR. Effect of increased adiposity on insulin sensitivity and adipokine concentrations in horses and ponies fed a high fat diet, with or without a once daily high glycaemic meal. *Equine Vet J*. 2016;48(3):368-373.

49. Cuadrado A, Nebreda AR. Mechanisms and functions of p38 MAPK signalling. *Biochem J*. 2010;429(3):403-417.

50. Leise BS, Yin C, Pettigrew A, Belknap JK. Proinflammatory cytokine responses of cultured equine keratinocytes to bacterial pathogen-associated molecular pattern motifs. *Equine Vet J*. 2010;42(4):294-303.

51. Lee M, Lee E, Jin SH, et al. Leptin regulates the pro-inflammatory response in human epidermal keratinocytes. *Arch Dermatol Res*. 2018; 310(4):351-362.

SUPPORTING INFORMATION

Additional supporting information may be found online in the Supporting Information section at the end of this article.